Journal Pre-proofs

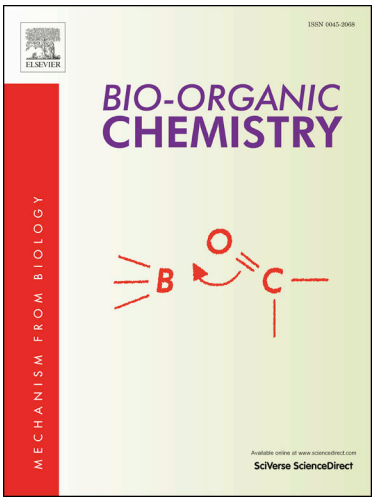

Design, synthesis and SARs of novel telomerase inhibitors based on BIBR1532

Chao Liu, Hua Zhou, Xiao Bao Sheng, Xin Hua Liu, Fei Hu Cheng

PII: S0045-2068(20)31374-2
DOI: https://doi.org/10.1016/j.bioorg.2020.104077
Reference: YBIOO 104077

To appear in: *Bioorganic Chemistry*

Received Date: 10 May 2020
Revised Date: 29 June 2020
Accepted Date: 3 July 2020

Please cite this article as: C. Liu, H. Zhou, X. Bao Sheng, X. Hua Liu, F. Hu Cheng, Design, synthesis and SARs of novel telomerase inhibitors based on BIBR1532, *Bioorganic Chemistry* (2020), doi: https://doi.org/10.1016/j.bioorg.2020.104077

Design, synthesis and SARs of novel telomerase inhibitors based on BIBR1532

Chao Liu[b,#], Hua Zhou [a,#], Xiao Bao Sheng[a], Xin Hua Liu[a,c]*, Fei Hu Cheng [c,]*

[a] *Engineering Research Center of Biomass Conversion and Pollution Prevention of Anhui Educational Institutions, Fuyang Normal University, Fuyang, 236037, P. R. China*

[b] *School of Chemistry and Chemical Engineering, Suzhou University, Suzhou, 234000, P. R. China*

[c] *School of Pharmacy, Anhui Medical University, Hefei, 230032, P. R. China*

Abstract: Telomerase has become one of the new popular targets for the development of anti-tumor drugs. Based on the structural characteristics of the BIBR1532 which has entered the stage of clinical research, six series total of 64 new compounds with diverse structural characteristics were designed and synthesized. The inhibitory activity against SGC-7901, MGC-803, SMMC-7721, A375 and GES cell lines and their telomerase inhibitory activity were tested. Among them, eight compounds showed good activity against cancer cells, among them compounds **56**, **57** and **59** also showed low toxicity. Some of them showed excellent telomerase inhibitory activity with IC_{50} values ranging from 0.62 μM to 8.87 μM. Based on above, in depth structure-activity relationships were summarized, the compounds by replacing methyl group with cyanide and retaining amide moiety had good anti-tumor activity, moderate cytotoxicity, and better telomerase inhibitory activity. The results should be used for reference in BIBR1532-based structural optimization for further development of small molecule telomerase inhibitors.

Keywords: TERT inhibitor; BIBR1532; telomerase inhibitor; design; synthesis

[#]These authors contributed equally to this work. *Corresponding author.
E-mail: xhliuhx@163.com.(Xin-Hua Liu); fhchen@sohu.com (F.H. Chen).

1. Introduction

Telomerase is a kind of ribonucleoprotein complex based on endogenous RNA as template. Telomere reverse transcriptase (TERT), telomerase RNA (TR) and telomerase-associated protein are the main components of telomerase[1-4]. The expression of TERT and TR in cells are different. TR is extensively distributed in cell [5,6]. In most tumor cells, telomerase exhibits specific expression with the increase of content TERT[7-11]. The activation of telomerase can stop telomere reduction in the process of cancer cell replication. Therefore, inhibition of telomerase activity may promote telomere damage and eventually cause apoptosis of cancer cells. So, telomerase has become an efficiency and specific selectivity target for anticancer drugs [12].

Tertomotide, is the only clinical drug targeting telomerase which has been widely researched [13-15]. The gene medication telomerase-dependent oncolytic adenovirus (OBP-301) [16, 17] and G-quadruplex [18-23] stabilizing agent (Quarfloxin) [24] have also been being in clinical trials. Imetelstat [25-28] and BIBR1532[29] are two inhibitors targeting TERT in clinical trials. However, there are still some problems about them, such as the mechanisms of telomerase reactivation and inhibition remain is unclear, the toxic and side effect is universal. Therefore, development of new telomerase inhibitors, especially those with high specificity, high efficiency and longer half-life time, has always been the goal of our attention. Although BIBR1532, the first non-competitive telomerase inhibitor with high selectivity, but has no inhibitory effect against solid tumor cells, is still an ideal lead compound [30-34].

In this study, we employed the co-crystallization of telomerase and BIBR1532 to explore the pharmacophore model, and structures of six serials derivatives were designed based on the pharmacophore and frame of BIBR1532[35-36]. Their activities against anti-tumor and telomerase inhibitory effect, toxicity were carried out.

2. Results and discussion

2.1 Design

The co-crystal complex of BIBR1532 with tetrahymena telomerase (PDB ID: 5CQG) provides data support for pharmacophore-based drug design. The DS pharmacophore model of Discovery Studio 2018 software was used to calculate the pharmacophore information. In addition, the SARs of BIBR1532 analogues reported by Barma provides more pharmacophore information [36]. The results show that this pharmacophore contains four hydrophobic centers and one negatively charged center, and the exclusion volume is temporarily omitted (Figure 1). Aromatic groups and double bonds between them is necessary for activity, however, *cis*-trans isomerization has little effect on activity. Rigid substructures such as alkenyl, amino, *etc* are also pharmacophores. Electron withdrawing groups are detrimental to activity.

Figure 1

The cyano derivatives is an important optimization strategy for lead compound in drug design. The application of nitrile can enhance the interaction between the ligand and the target protein [37]. In order to investigate the effects of hydrophobic interaction and steric hindrance, different aromatic groups were introduced into the BIBR1532. Oxime is a common functional group for anticancer agents [38]. The oxime-substituted group is one of the bioisosteres of the amide α,β-unsaturated ketone [39-41], which is the dominant moiety in molecular design. Based on the above information, and with classic medicinal chemistry methods, including fragment reduction, active fragment growth, cyclization, molecular hybridization, and bioisostere were applied to construct compound library. Six types (Figure 2) BIBR1532 derivatives were designed, their anticancer and telomerase inhibitory activities were investigated.

Figure 2

Based on the information observed from pharmacophore model, modifications of BIBR1532 were carried out in different manner (Figure 3). First, through the strategy of non-pharmacophore fragment reduction, compounds **1**~**10** with α,β-unsaturated ketone were designed and synthesized. Unfortunately, these compounds have poor anti-tumor activity except compound **5**. We speculated that the presence of nitrogen had important significance in anti-tumor effect and telomerase inhibitory activity. Next, the bioisostere strategy was applied to obtain compound **11**, which had good telomerase inhibitory and anti-tumor activity. Then, the application of the pharmacophore fragment growth strategy led to the compounds **16**~**25**. Compound **21** was an excellent compound with moderate telomerase activity. Considering that benzofuran and dihydropyrazole are valuable fragments, molecular splicing and cyclization strategies were applied to get compound **21**, then leading to the emergence of compounds **26**~**34**. Unfortunately, compounds with poor activity obtained by this strategy. In addition, the replacement of methyl hydrophobic center is another modification strategy. By replacing the methyl group with cyanide and retaining the amide moiety, compound **38** was synthesized, which was a valuable molecule for next modification. Finally, compound **56** was synthesized by halogen modification, ethyl substitution. By cyclization strategy, compound **59** was designed.

Figure 3

2.2 Chemistry

Total of 64 compounds were designed and synthesized. The compounds **1**~**10** were obtained by Witting reaction[42,43], carboxylic ester hydrolytic reaction[44,45] and Friedel-Crafts acylation[46, 47] (Scheme 1). The oximation of compounds **2**, **4**, **8**, **9**, **g1** could get compounds **11**~**15** [48,49]. In ethanol solution of sodium hydroxide, compounds **a1**~**a7** reacted with compounds **e1**~**e3** through Aldol condensation to get compounds **16**~**30**. Compound **25** or **h1** and hydrazide hydrate were refluxed in ethanol to obtain compounds **f1**, **f2** [50,51]. Compounds **f1**, **f2** reacted with the acyl

chloride to form compounds **31**~**34**. Started from aryl acetonitrile and glyoxylic acid monohydrate through condensation reaction [52,53] and amino-acid condensation reaction [54,55], the compounds **35**~**64** were synthesized (Scheme 2). Compounds **5** and **6** were determined by X-ray diffraction analysis through Bruker Smart APEX Ⅱ CCD (Figure 4 and Table 1).

Scheme 1

Scheme 2

Figure 4 and Table 1

2.3 SARs Studies

The anti-proliferative activity was determined with several human cancer cell lines, including SGC-7901, MGC-803, SMMC-7721and A375, adriamycin (ADR) used as positive control. Meanwhile, the human GES cell growth was used to assess the selectivity. Telomerase inhibitory activity was conducted by a modified TRAP assay [56], BIBR1532 and Staurosporin (STSN) were served as the controls [51].

The pharmacophore information and co-crystal of BIBR1532 indicated that the carboxyl group on the benzene ring could be replaced with other moiety, and the amide moiety does not seem to be necessary for activity. Therefore, compounds **1**~**10** with α, β-unsaturated ketone were first designed and synthesized (Figure 5). Compared with BIBR1532, these compounds retained hydrophobic center, but lacked the negatively charged center. Unfortunately, these compounds had poor anti-tumor activity (IC_{50} >100 μM). But, compound **5** showed good telomerase inhibitory activity with IC_{50} = 1.46 μM, which was much stronger than that of STSN (IC_{50} = 6.98 μM) (Table 2).

Figure 5

Table 2

Although the N atom of BIBR1532 was not included in the pharmacophore model, but, the presence of nitrogen should be show important significance against telomerase inhibitory activity (Figure 6). Therefore, by replacing the keto (C=O) moiety with oxime (C=NOH), we synthesized compounds **11**~**15**. Compared to α,β-unsaturated ketone, compounds **11**~**15** showed moderate or even better activity. Consistent with the inhibition of tumor proliferation, compounds **11**~**15** had good telomerase inhibitory activity (IC_{50} = 0.99~6.33 μM). Among them, compound **11** was the most one with good anti-tumor effect (IC_{50} = 2.84~10.79 μM) and telomerase inhibition activity (IC_{50} = 0.99 μM) (Table 3). Therefore, nitrogen seems to be a necessary moiety.

Figure 6

Table 3

Double bond between aromatic groups is necessary for activity. We then modified compound **1**, introduced additional double bond to form a conjugated olefin structure, compounds **16**~**25** were synthesized (Figure 7). The results showed substituent groups on the benzene ring had a significant effect on antitumor activity. By introducing an electron-withdrawing group or an electron-donating group or F on the benzene ring of one side, we obtained compounds **16**, **17**, **19** and **20**. But, only compound **20** showed moderate anti-tumor activity with no telomerase activity. By introducing different substituent groups on the benzene ring of the other side (**16**, **19**), compounds **22**~**24** were designed. Compared to compound **19**, compound **22** showed moderate inhibitory activity against tumor cells. The methoxy-substitution on the benzene ring could affect activity. Among them, when both phenyl rings were substituted with methoxy, compound **21** showed the best antitumor activity (IC_{50} = 1.56~6.41 μM), but with severe cytotoxicity. With the same telomerase activity, the compound of *ortho*-methoxy-substituted had moderate antitumor activity and no obvious cytotoxicity (compound **22**,Table 4).

Figure 7

Table 4

Benzofuran and dihydropyrazole derivatives used as telomerase inhibitors have been reported in our previous studies [50]. Therefore, through molecular hybridization and ring formation strategy, benzofuran and pyrazole moieties were introduced into compound **23**, and compounds **26~34** were designed and synthesized (Figure 8). However, none of these compounds had antitumor activity (Table 5).

Figure 8

Table 5

The replacement of methyl hydrophobic center is another modification strategy. By replacing the methyl group with cyanide and retaining the amide structure, compounds **35~49** were designed (Figure 9). These compounds contained the same core with different substitutions (**35~42**), among them, compound **38** showed good anti-tumor activity (IC_{50} =5.64~17.82 μM), moderate cytotoxicity, and better telomerase inhibitory activity. Surprisingly, the strongest telomerase inhibitors, compounds **39** (IC_{50} = 0.62 μM) and **42** (IC_{50} = 0.81 μM) with no obvious antitumor activity. By replacing the naphthalene ring of compound **35** with benzene ring, compounds **43~49** were synthesized with no significant improvement at activity (Table 6).

Figure 9

Table 6

Substituting the NH may be a feasible strategy to improve the activity (Figure 10). Modificating compounds **35** and **43** with methyl gave compounds **50-52**. Surprisingly, the anti-tumor and telomerase activity of these compounds have been significantly improved. Such changes encouraged us to synthesize more

NH-substituted compounds. The compound **52/53** benzene ring was modified by halogen substitution to get compounds **55~57**, which showed far better anti-tumor effect than that of compound **52/53**. In addition, the substitution of halogen also affected telomerase activity. Compared to compounds **52~57**, it can be found that there is no significant difference between ethyl substitution and methyl substitution.

The cyclization strategy was applied to compound **53/51**, compounds **58~59/60~64** were designed and synthesized, reduced anti-tumor effects but with good telomerase activity was found. In short, among these compounds, compound **56** obtained by halogen modification, ethyl substitution and cyanide substitution was the best one (IC_{50} = 1.87~11.16 μM), while compound **59** through cyclization strategy and cyanide substitution was the best telomerase inhibitor (IC_{50} = 0.93 μM) (Table 7).

Figure 10

Table 7

2.4 Cell cycle analysis

Compound **39** had the strongest telomerase activity with IC_{50} of 0.62 μM and moderate inhibition of MGC-803 cells proliferation. To verify whether cell cycle arrest lead to decrease cell proliferation, we used flow cytometric analysis to measure the effect of compound **39** on induction of cell cycle. As shown in Figure 11, treatment with increasing concentrations of compound **39** for 48 h increased the G2/M and S phase distribution from 19.34% to 23.34% and 26.64% to 36.82%, whereas the G0/G1 phase distribution decreased from 56.02% to 39.84%, respectively. This suggested that compound **39** induced cell cycle arrest at G2/M and S phase delaying cells cycle progression.

Figure 11

2.5 *Cell apoptosis analysis*

To determine whether compound **39** meditated inhibition of proliferation was

related to apoptosis, MGC-803 cells was selected for examination of cell morphology changes. The Annexin V-FITC/PI apoptosis detection kit was used in cell apoptosis analysis. As shown in Figure 12, the first quadrant usually represents damaged cells which was induced by mechanical forces, environmental stimulus and so on; the second quadrant generally denotes later period apoptotic cells and necrotic cells; the third quadrant often represents early apoptotic cells; and the forth quadrant customarily denotes normal cells. The percentage of AnnexinV-FITC binding MGC-803 cells significantly increased from 7.06 % to 89.50 %, after treatment with increasing concentrations of compound **39**. The results demonstrated that compound **39** induced apoptosis of MGC-803 cells in a concentration-dependent way.

Figure 12

2.6 Down-regulated expression of TERT protein

To test whether compound **39** modulates the expression of the TERT protein, we used Western blot. As shown in Figure 13, treatment with different concentrations of compound **39** for 48 h (MGC-803 cells were selected), expression level of TERT protein was reduced. The result indicated compound **39** might be an efficiency regulator as TERT.

Figure 13

2.7 Docking study

Based on pharmacophore model in design section, molecular docking was further used to analyze the binding mode of compound **39** to TERT. The binding mode of the compound **39** is similar to BIBR1532 as shown in **Figure 14**. Naphthalene ring of the compound **39** and BIBR1532 generates interaction(compound **39**: *pi*-alkyl, BIBR1532: *pi*-sigma) with amino acid residues Leu554. Ile554 and Phe494 still retain the interaction with the benzene ring of small molecules. Carboxyl group as anion center is one of the pharmacophores in BIBR1532, Compound **39** lacks a negative

electron center. However, hydrogen bonding interactions with amino acid residues Arg486 make up for the lack of this pharmacophore. Meanwhile, the results of docking show that the interactions energy between compound **39**, BIBR1532 and TERT are -38.428 kcal/mol, -44.386 kcal/mol, respectively, which was consistent with the inhibitory activities of telomerase 0.62 μM and 0.32 μM.

Figure 14

3. Conclusions

With the aim to discover high efficiency telomerase inhibitors, based on rational design and follow-up strategy, total of 64 new BIBR1532 derivatives were designed and synthesized. Many of these compounds showed good inhibitory activity against tested cancer cells. Their structure-activity relationships were well summarized on basis of different design strategies. Especially, some title compounds (35-49), through replacement of methyl hydrophobic center, not only had strong inhibitory activity against telomerase, but also exhibited moderately effective antiproliferative activity against SGC-7901, MGC-803, SMMC-7721 and A375 cell lines, superior to that of BIBR1532, and it also showed non-toxic effects against human normal GES cell. Among them, Compound **39** showed the strongest telomerase inhibitory activity with IC_{50} of 0.62 μM and moderate inhibition of MGC-803 proliferation, which was selected for further mechanism study. The result indicated that MGC-803 cells cycle were arrested in the G2/M and S phase by this compound**,** thereby inducing MGC-803 cells apoptosis in a concentration-dependent way. Western blot revealed that compound **39** could decrease expression of TERT.

4. Experimental section

4.1 Chemistry

Adriamycin was purchased from Aladdin Chemical Reagent Co., Ltd (Shanghai, China), while thiazolyl blue and phosphate buffered saline were purchased from Beyotime Biotechnology (Shanghai, China). Other reagents were purchased from

Sigma-Aldrich (U.S.A) and Sinopharm Chemical Reagent Co., Ltd (Shanghai, China). ^{1}H NMR spectra were recorded on 400 MHz or 600 MHz and TMS or residual protio-solvent was used as internal standards. And chemical shifts were recorded relative to the solvent resonance ($CDCl_3$, 77.0 ppm). *General procedure for preparation and characterization of all compounds (See Support information).*

4.2 Crystallographic Studies

The diffraction data of the single crystal compounds were determined by Bruker Smart APEX Ⅱ CCD single Crystal diffractometer using MoKα radiation at 295 K in the range of $3.28^{o} \leq 2\theta \leq 55.18^{o}$. The obtained diffraction data were corrected and refined by the SADABS program of SHELXS-97 software with directive method and difference Fourier method. The anisotropy thermal parameters of all non-hydrogen atoms have been qualified by the method of least squaresost hoc Dunnett's test. In all cases, $p<0.05$ was considered statistically significant.

4.3 Cell Proliferation Assays

4.3.1 Cell Culture

The human tumor cell lines SGC-7901, MGC-803, SMMC-7721, A375 and human gastric epithelial cell GES were cultured in DMEM (dulbecco's modified eagle medium) contains 10% fetal bovine serum and double antibiotics (penicillin 100 IU/mL and streptomycin 0.1 mg/mL) and incubated at 37°C, 5% CO_2 atmosphere.

4.3.2 MTT Assays

Cells in logarithmic growth were digested with 0.25% trypsin, diluting to 1×10^{4}/mL cell suspension with the complete medium. The cells were seeded in 96 well plates with 100 μL cell suspension per well and incubated at 37°C and 5% CO_2 atmosphere. After 24 h, the medium was discarded and each well was added 100 μL medium containing tested compounds. The BIBR1532 as a positive reference and the wells without cells as blank control group. After 48 h exposure period,25 μL of PBS containing 2.5 mg/mL of MTT was added to each well. After 4 h, the medium was

discarded and 150 μL DMSO were added to dissolve the purple formazan crystals produced. The absorbance were measured at 492 nm on an ELISA plate reader. The data represented the mean of three experiments in triplicate and were expressed as means±SD using Student *t* test. The IC_{50} value was defined as the concentration at which 50% of the cells could survive.

4.4 Telomerase Activity Assays

Human gastric cancer cell line MGC-803 was used to detect telomerase activity. Cells in logarithmic phase were transferred into flasks and cultured until adherence. The compounds to be detected were divided into 7 groups with a concentration ranged from 60 to 0.08mg/mL. Treated after 24 hours, the cells was collected and washed PBS. The inhibitory effects of compounds about telomerase were tested through TRAP-PCR-ELISA. Each 50 μL TRAP reaction mixture contained 115 mM $MgCl_2$, 63 mM KCl, 1 mM EGTA, 0.005% Tween-20, 20 mM tris-HCl (pH 8.3), 0.1 μg TS primer, 50 μM dNTP (deoxy-ribonucleoside triphosphate), 0.1 mg/mL bovine serum albumin (BSA) and 1 μg T4 Gene 32 Protein, 1~2 μL CHAPS cell extract protein(6 μg), 0.2~0.4 μL [α-32P] dGIP. After incubation for 10 minutes at 23 ^oC, inactivation was performed at 94 ^oC for 30 seconds, followed by addition of 0.1 μg cX and 2U Taq, the reaction mixture with 27 PCR cycles were repeated at 94 ^oC 30 s, 50 ^oC 30 s, 72 ^oC 1.5 min. 25 μL of the product was collected and detected by polyacrylamide gel electrophoresis (PAGE). The results was evaluated via microplate reader.

4.6 Cell cycle assay

For cell cycle analysis, cell cycle kit (Beyotime, China) was performed. MGC-803 cells were treated with compound **39** at different concentrations as 7, 14, 28 μM for 48 h. Untreated and treated cells were harvested, and then MGC-803 cells were washed three times by cold PBS. And then cells were fixed in 70% ethanol at -20°C for 1 h. After fixation, cells were washed with cold PBS and stained with 0.5 mL of propidium iodide (PI) staining buffer, which contain 200 mg/mL RNase A and 50 μg/mL PI, at 37°C for 30 min in the dark. Analyses were performed on a BD

FACS Verse Flow Cytometer. The experiments were repeated three times.

4.7 Apoptosis assay

For cell apoptosis analysis by annexin V-FITC/PI apoptosis detection kit (BestBio, China). MGC-803 cells in logarithmic growth phase were treated with compound **39** at different concentrations as 7, 14, 28 μM for 48 h. Cells were collected in cold PBS by centrifugation for 5 min at 1000 g. And then cells were re-suspended at a buffer, stained with FITC-labeled annexin V and PI for 20 min and immediately analyzed on a BD FACS Verse Flow Cytometer.

4.8 Western blotting

Human MGC-803 cells were lysed with RIPA lysis buffer (Beyotime, China). Whole extracts were prepared,and protein concentration was detected using a BCA protein assay kit (Beyotime, China). The protein samples were separated by SDS-PAGE and blotted onto a PVDF membrane (Millipore Corp, Billerica, MA, USA). After blockade of nonspecific protein binding, nitrocellulose blots were incubated at 4°C for 8 h with primary antibodies. TERT was used as was anti-β-actin (proteintech, USA). After extensive washing in TBS/Tween-20, the membranes were incubated at room temperature for 1 h with secondary antibodies. Anti-mouse combined with horseradish peroxidase as secondary antibodies. After washed in TBS/Tween-20, the blots were processed with distilled water for detection of antigen using the enhanced chemiluminescence system. Proteins were visualized with ECL-chemiluminescent kit (ECL-plus, Thermo Scientific).

Supporting Information

The following files are available free. Some NMR and HRMS.

Acknowledgments

This work was supported by the National Natural Science Funding of China (21977001). The authors wish to thank the Horizontal cooperation project of Fuyang

municipal government (No. XDHX201722 and XDHX2016026), Horizontal cooperation project of Yifan Pharmaceutical Co., Ltd (HX2019033).

Reference

[1] C.W. Greider, E.H. Blackburn, Identification of a specific telomere terminal transferase activity in tetrahymena extracts, Cell, 43 (1985) 405-413.

[2] C.W. Greider, E.H. Blackburn, A telomeric sequence in the RNA of Tetrahymena telomerase required for telomere repeat synthesis, Nature, 337 (1989) 331-337.

[3] H. Chan, Y. Wang, J. Feigon, Progress in Human and Tetrahymena Telomerase Structure Determination, Annu Rev Biophys, 46 (2017) 199-225.

[4] T.H.D. Nguyen, J. Tam, R.A. Wu, B.J. Greber, D. Toso, E. Nogales, K. Collins, Cryo-EM structure of substrate-bound human telomerase holoenzyme, Nature, 557 (2018) 190-195.

[5] T. Lange, De Lange, T. Protection of mammalian telomeres. Oncogene 21, 532-540, Oncogene, 21 (2002) 532-540.

[6] W.C. Hahn, S.A. Stewart, M.W. Brooks, S.G. York, E. Eaton, A. Kurachi, R.L. Beijersbergen, J.H.M. Knoll, M. Meyerson, R.A. Weinberg, Inhibition of telomerase limits the growth of human cancer cells, Nature Medicine, 10 (1999) 1164-1170.

[7] A survey of telomerase activity in human cancer, European Journal of Cancer, 33 (1997) 787-791.

[8] J. Griffith, Telomerase activity in human cancer, Current Opinion in Oncology, 8 (1996) 66-71.

[9] A.J. Cesare, R.R. Reddel, Alternative lengthening of telomeres: models, mechanisms and implications, Nature Reviews Genetics, 11 (2010) 319-330.

[10] Y. Cao, T.M. Bryan, R.R. Reddel, Increased copy number of the TERT and TERC telomerase subunit genes in cancer cells, Cancer Science, 99 (2008) 1092-1099.

[11] Y. Y. Li, G.J. Pan, Y. Chen, Q. Yang, T.T. Hao, L.B. Zhao, L. Zhao, Y.S. Cong, A.P. Diao, P. Yu, Inhibitor of the human telomerase reverse trancriptase (hTERT) gene promoter induces cell apoptosis via a mitochondrial-dependent pathway, Eur J

Med Chem, 145 (2018) 370-378.

[12] J.W. Shay, Telomerase: a target for cancer therapeutics, Cancer Cell, 2 (2002) 257-265.

[13] S. Caroline, M. Fariba, F.D. Jan-Erik, M. H?Kan, L. Maria, Telomerase (GV1001) vaccination together with gemcitabine in advanced pancreatic cancer patients, International Journal of Oncology, 45 (2014) 1293-1303.

[14] J.K. Park, Y. Kim, H. Kim, J. Jeon, T.W. Kim, J.H. Park, Y.I. Hwnag, W.J. Lee, J.S. Kang, The anti-fibrotic effect of GV1001 combined with gemcitabine on treatment of pancreatic ductal adenocarcinoma, Oncotarget, 7 (2016) 75081-75093.

[15] Y.K. Lee, B.S. Nata'atmaja, B.H. Kim, C.S. Pak, C.Y. Heo, Protective effect of telomerase-based 16-mer peptide vaccine (GV1001) on inferior epigastric island skin flap survivability in ischaemia-reperfusion injury rat model, Journal of Plastic Surgery and Hand Surgery, 51 (2017) 210-216.

[16] S. Tanabe, H. Tazawa, S. Kagawa, K. Noma, K. Takehara, T. Koujima, H. Kashima, T. Kato, S. Kuroda, S. Kikuchi, Abstract CT123: Phase I/II trial of endoscopic intratumoral administration of OBP-301, a novel telomerase-specific oncolytic virus, with radiation in elderly esophageal cancer patients, Cancer Research, 75 (2015) CT123-CT123.

[17] T. Kojima, T. Fujiwara, Y. Shirakawa, H. Ono, M. Nakamoto, H. Hasegawa, N. Hirano, M. Wakabayashi, S. Nomura, Y. Togashi, H. Nishikawa, A. Sato, A. Ohtsu, T. Doi, An open label phase I study to evaluate the safety and efficacy of OBP-301 with pembrolizumab in patients with advanced solid tumors, Journal of Clinical Oncology, 36 (2018) TPS3117-TPS3117.

[18] S. Bhattacharya, P. Chaudhuri, A. K. Jain, P. Ananya, Symmetrical bisbenzimidazoles with benzenediyl spacer: the role of the shape of the ligand on the stabilization and structural alterations in telomeric G-quadruplex DNA and telomerase inhibition, Bioconjug Chem, 21 (2010) 1148-1159.

[19] K. Zhou, J.C. Liu, X.Q. Xiong, M. Cheng, X.L. Hu, S. Narva, X.Y. Zhao, Y.L.Wu, W. Zhang, Design, synthesis of 4,5-diazafluorene derivatives and their anticancer activity via targeting telomeric DNA G-quadruplex. Eur J Med Chem, 178

(2019) 484-499.

[20] M. Recagni, M. L. Greco, A. Milelli, A. Minarini, N. Zaffaroni, M. Folini, C. Sissi, Distinct biological responses of metastatic castration resistant prostate cancer cells upon exposure to G-quadruplex interacting naphthalenediimide derivatives, Eur J Med Chem, 177 (2019) 401-413.

[21] Specific Stabilization of Promoter G-Quadruplex DNA by 2,6-Disubstituted Amidoanthracene-9,10-dione based Dimeric Distamycin Analogues and their Selective Cancer Cell Cytotoxicity, S. Roy, A. Ali, M. Kamra, K. Muniyappa, S. Bhattacharya, Eur J Med Chem, 2020, doi.org/10.1016/j.ejmech.2020.112202.

[22] Q.P. Qin, Z.F. Chen, W.Y. Shen, Y.H. Jiang, D. Cao, Y.L. Li, Q.M. Xu, Y.C. Liu, K.B. Huang, H. Liang, Synthesis of a platinum(II) complex with 2-(4-methoxyphenyl) imidazo [4,5f]-[1,10] phenanthrolin and study of its antitumor activity, Eur J Med Chem, 89 (2015) 77-87.

[23] Z.F. Chen, Q.P. Qin, J.L. Qin, Y.C. Liu, K.B. Huang, Y.L. Li, T. Meng, G.H. Zhang, Y. Peng, J. Luo, H. Liang, Stabilization of G-quadruplex DNA, inhibition of telomerase activity and tumor cell apoptosis of organoplatinum(II) complexes with oxoisoaporphine, J Med Chem, 58 (2015) 2159-2179.

[24] J. Bidzinska, G. Cimino-Reale, N. Zaffaroni, M. Folini, G-Quadruplex Structures in the Human Genome as Novel Therapeutic Targets, Molecules (Basel, Switzerland), 18 (2013) 12368-12395.

[25] T. Ayalew, T.L. Lasho, K.H. Begna, M.M. Patnaik, D.L. Zblewski, C.M. Finke, R.R. Laborde, W. Emnet, S. Lauren, C.A. Hanson, A Pilot Study of the Telomerase Inhibitor Imetelstat for Myelofibrosis, N Engl J Med, 373 (2015) 908-919.

[26] A.A. Chiappori, T. Kolevska, D.R. Spigel, S. Hager, M. Rarick, S. Gadgeel, N. Blais, J. Pawel, Von, L. Hart, M. Reck, A randomized phase II study of the telomerase inhibitor imetelstat as maintenance therapy for advanced non-small-cell lung cancer, Annals of Oncology, 26 (2015) 354-362.

[27] R. Salloum, T.R. Hummel, S.S. Kumar, K. Dorris, S. Li, T. Lin, V.M. Daryani, C.F. Stewart, L. Miles, T.Y. Poussaint, A molecular biology and phase II study of imetelstat (GRN163L) in children with recurrent or refractory central nervous system

malignancies: a pediatric brain tumor consortium study, Journal of Neuro-Oncology, 129 (2016) 443-451.

[28] J. Mascarenhas, R.S. Komrokji, M. Cavo, B. Martino, D. Niederwieser, A. Reiter, B.L. Scott, M.R. Baer, R. Hoffman, O. Odenike, J. Bussolari, E. Zhu, F. Huang, E. Rose, L. Sherman, S. Dougherty, F.M. Feller, J.-J. Kiladjian, Imetelstat Is Effective Treatment for Patients with Intermediate-2 or High-Risk Myelofibrosis Who Have Relapsed on or Are Refractory to Janus Kinase Inhibitor Therapy: Results of a Phase 2 Randomized Study of Two Dose Levels, Blood, 132 (2018) 685.

[29] K. Damm, U. Hemmann, P. Garin-Chesa, N. Hauel, I. Kauffmann, H. Priepke, C. Niestroj, C. Daiber, B. Enenkel, B. Guilliard, I. Lauritsch, E. Muller, E. Pascolo, G. Sauter, M. Pantic, U.M. Martens, C. Wenz, J. Lingner, N. Kraut, W.J. Rettig, A. Schnapp, A highly selective telomerase inhibitor limiting human cancer cell proliferation, The EMBO journal, 20 (2001) 6958-6968.

[30] P. Emanuelle, W. Christian, L. Joachim, H. Norbert, P. Henning, K. Iris, G.C. Pilar, W.J. Rettig, D. Klaus, S. Andreas, Mechanism of human telomerase inhibition by BIBR1532, a synthetic, non-nucleosidic drug candidate, Journal of Biological Chemistry, 277 (2002) 15566-15572.

[31] H. El-Daly, M. Kull, S. Zimmermann, M. Pantic, C.F. Waller, U.M. Martens, Selective cytotoxicity and telomere damage in leukemia cells using the telomerase inhibitor BIBR1532, Blood, 105 (2005) 1742-1749.

[32] C. Bryan, C. Rice, H. Hoffman, M. Harkisheimer, M. Sweeney, E. Skordalakes, Structural Basis of Telomerase Inhibition by the Highly Specific BIBR1532, Structure, 23 (2015) 1934-1942.

[33] F. Doğan, N.P. Özateş, B.G. Bağca, Z. Abbaszadeh, F. Söğütlü, R. Gasımlı, C. Gündüz, Ç. Biray Avcı, Investigation of the effect of telomerase inhibitor BIBR1532 on breast cancer and breast cancer stem cells, Journal of Cellular Biochemistry, 120 (2019) 1282-1293.

[34] A. Pourbagheri-Sigaroodi, D. Bashash, A. Safaroghli-Azar, M. Farshi-Paraasghari, M. Momeny, F.N. Mansoor, S.H. Ghaffari, Contributory role of microRNAs in anti-cancer effects of small molecule inhibitor of telomerase

(BIBR1532) on acute promyelocytic leukemia cell line, European Journal of Pharmacology, 846 (2019) 49-62.

[35] C. Liao, M. Sitzmann, A. Pugliese, M.C. Nicklaus, Software and resources for computational medicinal chemistry, Future Medicinal Chemistry, 3 (2011) 1057-1085.

[36] D.K. Barma, A. Elayadi, J.R. Falck, D.R. Corey, Inhibition of telomerase by BIBR 1532 and related analogues, Bioorganic & Medicinal Chemistry Letters, 13 (2003) 1333-1336.

[37] F.F. Fleming, L. Yao, P.C. Ravikumar, L. Funk, B.C. Shook, Nitrile-Containing Pharmaceuticals: Efficacious Roles of the Nitrile Pharmacophore, J Med Chem, 53 (2010) 7902-7917.

[38] D.A. Rodrigues, G.À. Ferreira-Silva, A.C.S. Ferreira, R.A. Fernandes, J.K. Kwee, C.M.R. Sant'Anna, M. Ionta, C.A.M. Fraga, Design, Synthesis, and Pharmacological Evaluation of Novel N-Acylhydrazone Derivatives as Potent Histone Deacetylase 6/8 Dual Inhibitors, J Med Chem, 59 (2016) 655-670.

[39] C. Seidel, M. Schnekenburger, C. Zwergel, F. Gaascht, A. Mai, M. Dicato, G. Kirsch, S. Valente, M. Diederich, Novel inhibitors of human histone deacetylases: Design, synthesis and bioactivity of 3-alkenoylcoumarines, Bioorganic & Medicinal Chemistry Letters, 24 (2014) 3797-3801.

[40] Z. Baoxin, D. Dongzhu, G. Chunpo, Y. Juan, L. Yaping, L. Xinming, F. Jianguo, Synthesis of xanthohumol analogues and discovery of potent thioredoxin reductase inhibitor as potential anticancer agent, J Med Chem, 58 (2015) 1795-1805.

[41] D.K. Mahapatra, S.K. Bharti, V. Asati, Anti-cancer chalcones: Structural and molecular target perspectives, Eur J Med Chem, 46 (2015) 69-114.

[42] Z.C. Duan, X.P. Hu, C. Zhang, Z. Zheng, Enantioselective Rh-Catalyzed Hydrogenation of 3-Aryl-4-phosphonobutenoates with a P-Stereogenic BoPhoz-Type Ligand, The Journal of Organic Chemistry, 75 (2010) 8319-8321.

[43] D. Jun, D. Zheng-Chao, H. Jia-Di, H. Xiang-Ping, W. Dao-Yong, Y. Sai-Bo, X. Xue-Feng, Z. Zhuo, Rh-catalyzed asymmetric hydrogenation of gamma-phthalimido-substituted alpha,beta-unsaturated carboxylic acid esters: an

efficient enantioselective synthesis of beta-aryl-gamma-amino acids, Organic Letters, 9 (2007) 4825-4828.

[44] P.K. Mandal, G. Fengqin, L. Zhen, R. Zhiyong, R. Rajagopal, B. J Sanderson, K.K. Kaluarachchi, C. Xiaomin, R.C. Bast, W.S. Liao, Potent and selective phosphopeptide mimetic prodrugs targeted to the Src homology 2 (SH2) domain of signal transducer and activator of transcription 3, J Med Chem, 54 (2011) 3549-3563.

[45] M. Ogino, Y. Nakada, N. Negoro, S. Itokawa, S. Nishimura, T. Sanada, T. Satomi, S. Kita, K. Kubo, S. Marui, Discovery of a Novel Acyl-CoA: Cholesterol Acyltransferase Inhibitor: The Synthesis, Biological Evaluation, and Reduced Adrenal Toxicity of (4-Phenylcoumarin)acetanilide Derivatives with a Carboxylic Acid Moiety, Chemical and Pharmaceutical Bulletin, 59 (2011) 1369-1375.

[46] J.P. Grealis, H. Müller-Bunz, Y. Ortin, M. Casey, M.J. Mcglinchey, Synthesis of Isobavachalcone and Some Organometallic Derivatives, European Journal of Organic Chemistry, 2013 (2013) 332-347.

[47] T. Keumi, T. Inagaki, N. Nakayama, M. Taniguchi, T. Morita, H. Kitajima, Ortho-selective side-chain nitration of methyl-substituted alkenoylbenzenes and its application to synthesis of 4-nitro-1-tetralones, The Journal of Organic Chemistry, 54 (1989) 4034-4038.

[48] S. Liu, L.S. Liebeskind, A Simple, Modular Synthesis of Substituted Pyridines, Journal of the American Chemical Society, 130 (2008) 6918-6919.

[49] X. Zhu, Y.F. Wang, W. Ren, F.L. Zhang, S. Chiba, TEMPO-Mediated Aliphatic C–H Oxidation with Oximes and Hydrazones, Organic Letters, 15 (2013) 3214-3217.

[50] X. H. Liu, J. Li, B. A. Song, X. B. Qi, Design and synthesis of novel 5-phenyl-N-piperidine ethanone containing 4,5-dihydropyrazole derivatives as potential antitumor agents, Eur J Med Chem, 51 (2012) 294-299.

[51] Y. Wang, F.X. Cheng, X.L. Yuan, W.J. Tang, J.B. Shi, C.Z. Liao, X. H. Liu, Dihydropyrazole derivatives as telomerase inhibitors: Structure-based design, synthesis, SAR and anticancer evaluation in vitro and in *vivo*, Eur J Med Chem, 112 (2016) 231-251.

[52] W.D. Dean, D.M. Blum, Condensation of Arylacetonitriles with Glyoxylic Acid.

Facile Synthesis of Arylmaleic Acid Derivatives, The Journal of Organic Chemistry, 58 (1993) 7916-7917.

[53] B.M. Fox, K. Iio, K. Li, R. Choi, T. Inaba, S. Jackson, S. Sagawa, B. Shan, M. Tanaka, A. Yoshida, F. Kayser, Discovery of pyrrolopyridazines as novel DGAT1 inhibitors, Bioorganic & Medicinal Chemistry Letters, 20 (2010) 6030-6033.

[54] L. Qiang, Y. Ya-Ting, C. Chang-Shi, D. Melanie, J.C. Byrd, M.R. Etherton, U. Asad, C. Ching-Shih, Zn2+-chelating motif-tethered short-chain fatty acids as a novel class of histone deacetylase inhibitors, J Med Chem, 47 (2004) 467-474.

[55] J. Jae-Chul, M. Sohyeon, M. Dongguk, P. Woo Kyu, J. Mankil, O. Seikwan, Synthesis and evaluation of a series of 3,4,5-trimethoxycinnamic acid derivatives as potential antinarcotic agents, Chemical Biology & Drug Design, 81 (2013) 389-398.

[56] H. Han, L.H. Hurley, M. Salazar, A DNA polymerase stop assay for G-quadruplex-interactive compounds, Nucleic Acids Research, 27 (1999) 537-542.

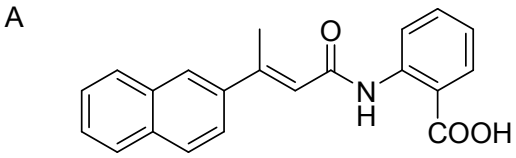

BIBR1532 IC_{50} = 0.093 μM

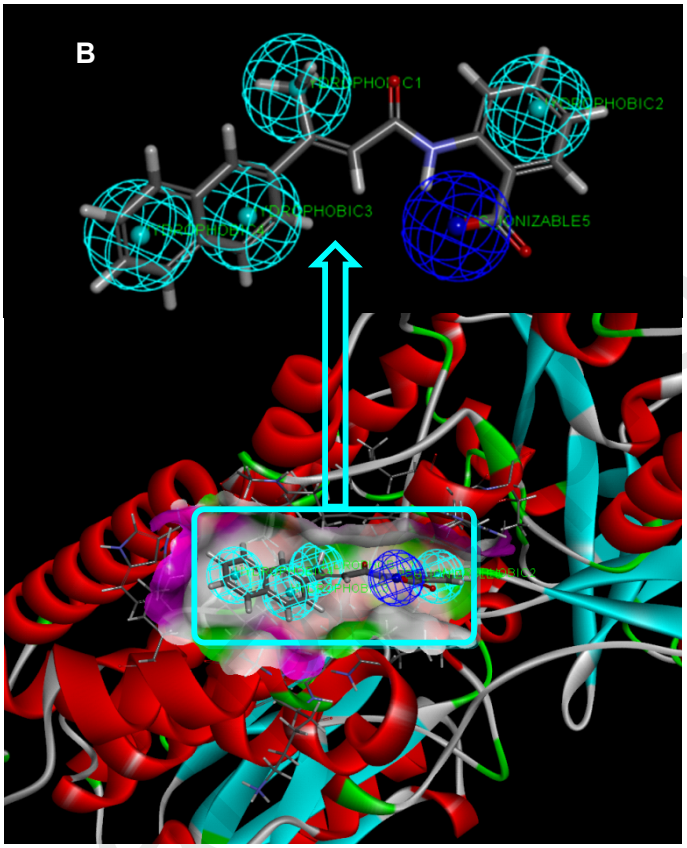

Figure 1. (A) Chemical structure of BIBR1532; (B) Pharmacophore of complex

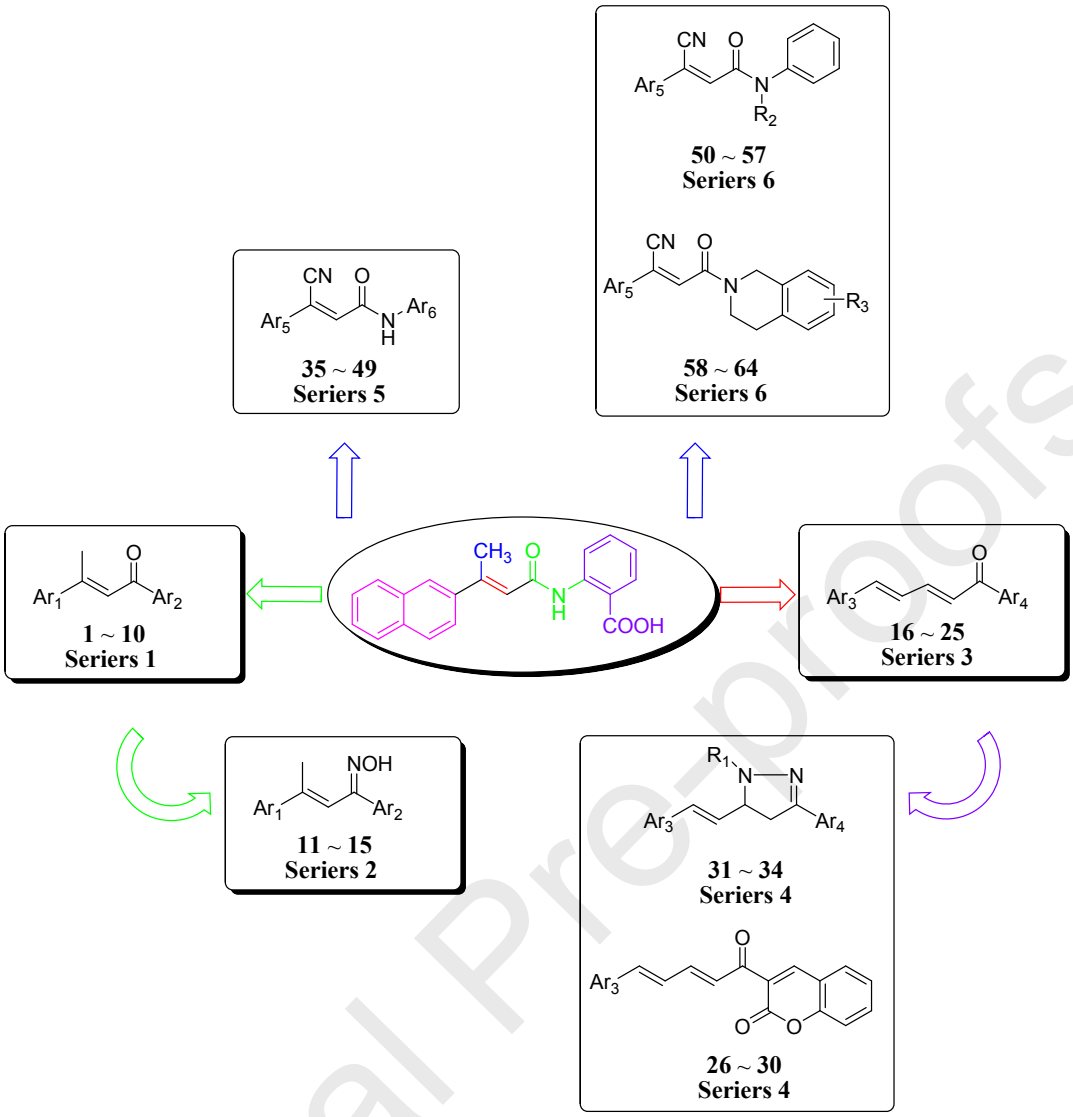

Figure 2. The workflow of the general design strategy in this study

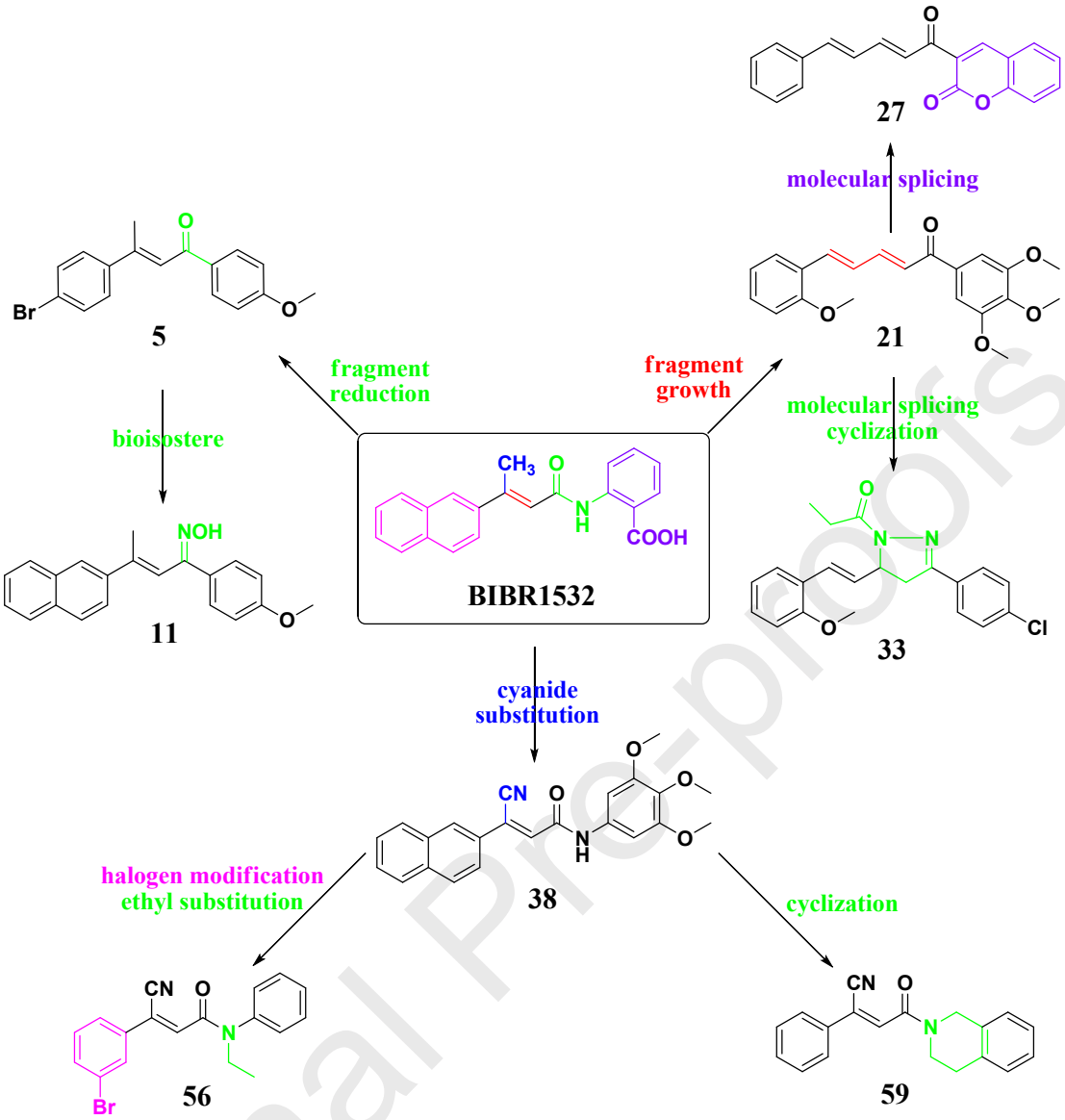

Figure 3. Representative active compounds of different strategies

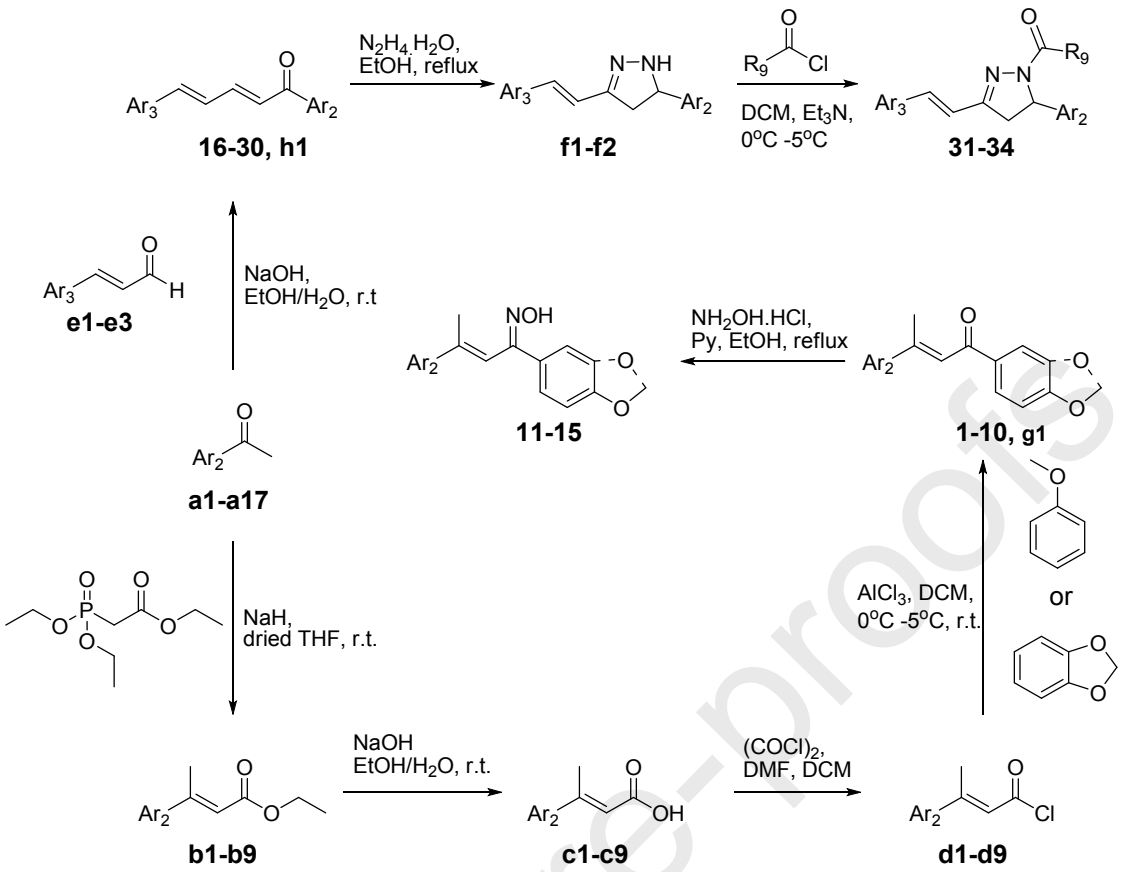

Scheme 1. Synthesis of compounds **1**~**34**

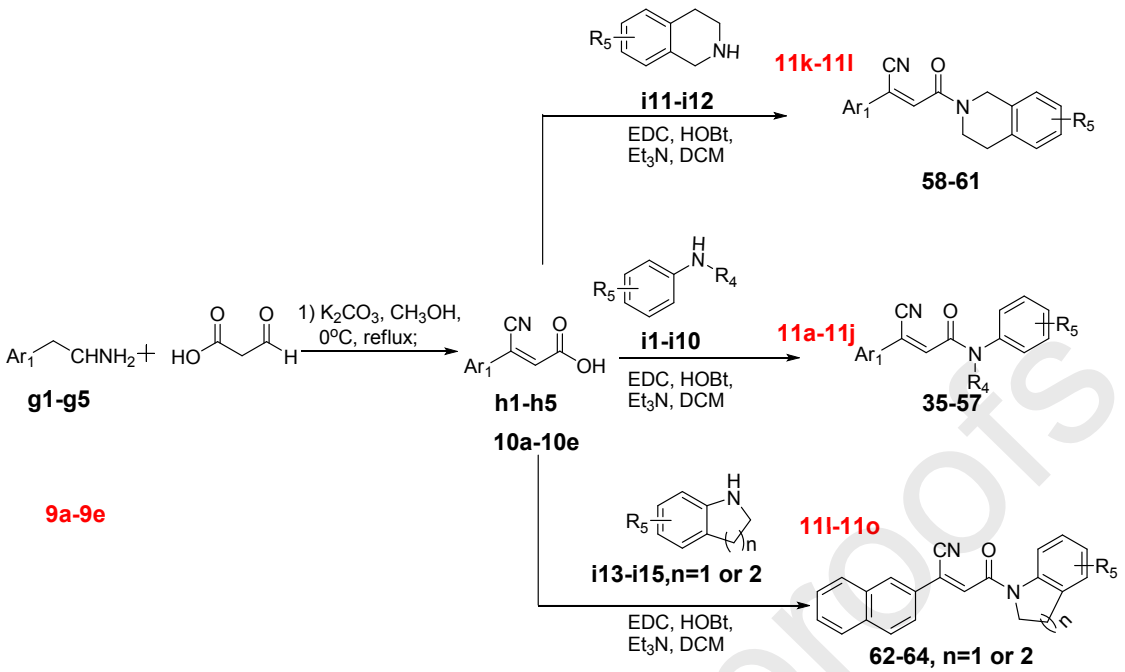

Scheme 2. Synthesis of compounds **35~64**

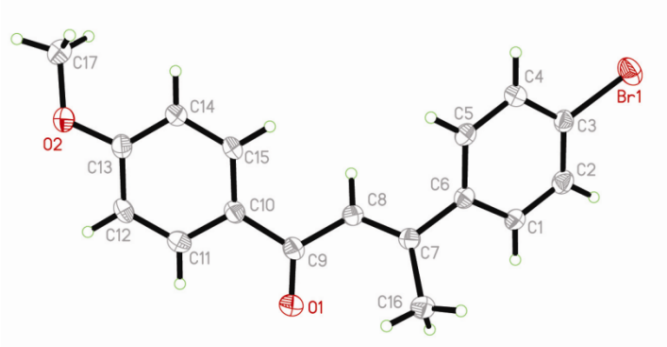

A

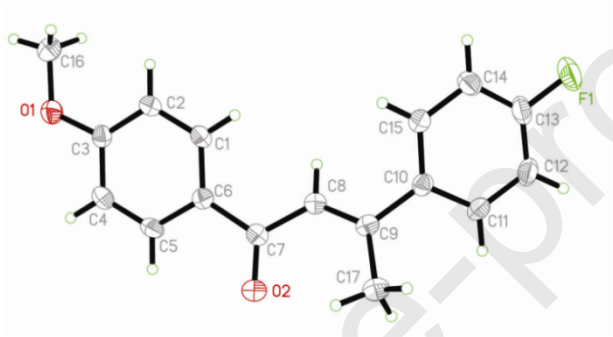

B

Figure 4. ORTEP drawing of compounds **5** and **6**

Table 1. Crystallographical data of compounds **5** and **6**

Properties	**5**	**6**
Chemical formula	$C_{17}H_{15}BrO_2$	$C_{17}H_{15}FO_2$
Formula weight	331.20	270.29
Temperature/K	294.86(10)	294.69(12)
Crystal system	monoclinic	monoclinic
Space group	$P2_1/c$	Pc
a/Å	6.1731(3)	6.1980(4)
b/Å	32.1856(14)	15.5726(10)
c/Å	7.4898(4)	7.3323(7)
α/°	90	90
β/°	103.897(4)	104.705(8)
γ/°	90	90
V/Å^3	1444.57(12)	684.52(9)
ρ_{calc}g/cm^3	1.523	1.311
Z	4	2
λ (MoKα)	0.71073	0.71073
F(000)	672.0	284.0
θ range(^{0})	6.77 to 52.032	6.796 to 52.042
Index ranges	$-7 \le h \le 6$, $-29 \le k \le 39$, $-9 \le l \le 8$	$-7 \le h \le 6$, $-14 \le k \le 19$, $-9 \le l \le 8$
Reflections collected	4847	2531
Independent reflections	2849 [R_{int} = 0.0260, R_{sigma} = 0.0533]	1828 [R_{int} = 0.0246, R_{sigma} = 0.0452]
Data/restraints/parameters	2849/0/183	1828/2/183
Goodness-of-fit on F^2	1.061	1.096

Final R indexes [I>=2σ (I)	R_1 = 0.0509, wR_2 = 0.0973	R_1 = 0.0465, wR_2 = 0.0907
Final R indexes [all data]	R_1 = 0.0768, wR_2 = 0.1082	R_1 = 0.0644, wR_2 = 0.1014
Largest diff. peak/hole / e $Å^{-3}$	0.62/-0.36	0.17/-0.19
Flack parameter	/	0.4(10)

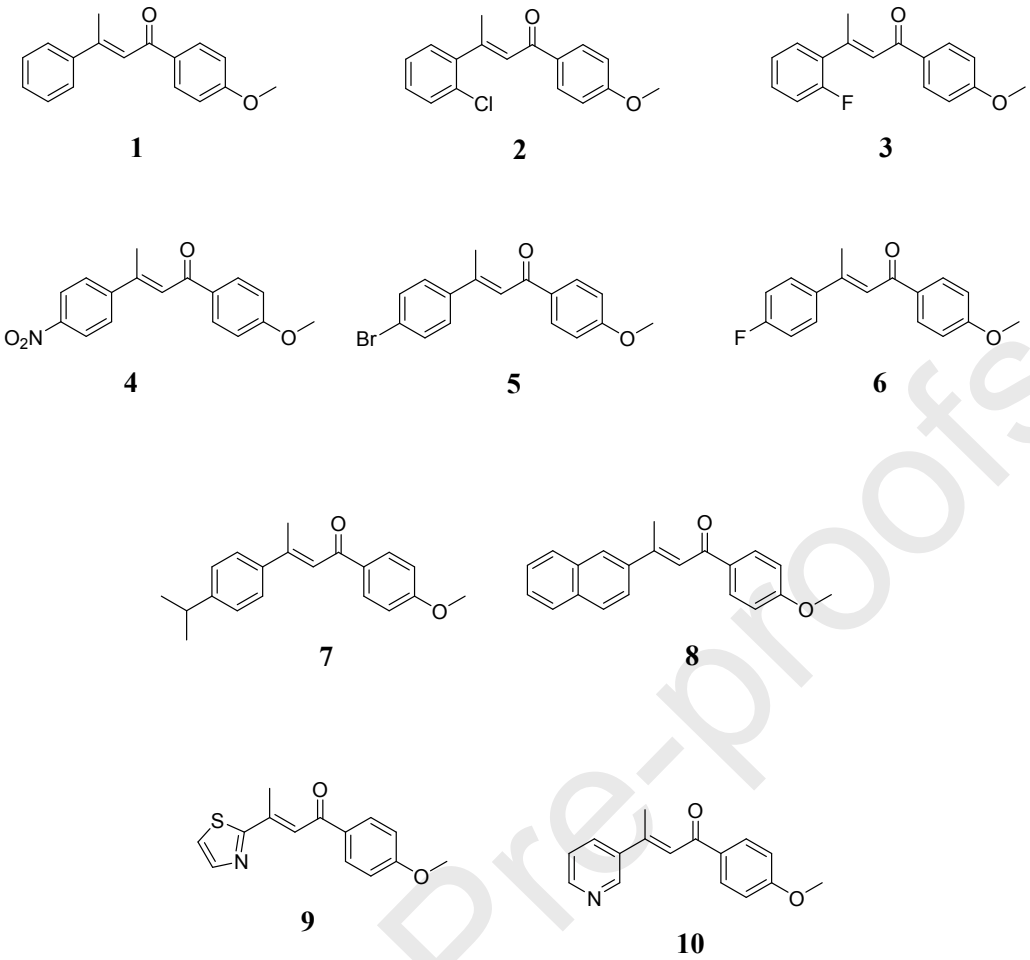

Figure 5. The structure of compounds **1~10**

Table 2. Inhibitory activities of compounds **1**~**10** against SGC-7901, A375, SMMC-7721, MGC-803, GES cell lines [a] and telomerase [b]

compound	IC_{50}（μM）					
	SGC-7901	A375	SMMC-7721	MGC-803	GES	telomerase
1	>100	>100	>100	>100	>100	ND[d]
2	>100	>100	>100	>100	>100	8.87±1.37
3	>100	>100	>100	>100	>100	-[e]
4	>100	>100	>100	>100	>100	-
5	63.21±4.39	65.17±3.73	>100	30.75±3.72	73.48±4.01	1.46±0.33
6	>100	>100	>100	>100	>100	ND
7	>100	>100	>100	>100	>100	-
8	>100	>100	>100	>100	>100	ND
9	>100	>100	>100	>100	>100	-
10	>100	>100	>100	>100	>100	-
ADR[c]	0.62±0.21	0.75±0.23	0.55±0.36	0.84±0.094	0.69±0.30	-
STSN[c]	-	-	-	-	-	6.98±1.59
BIBR1532[c]	-	-	-	-	-	0.32±0.07

[a] The data represented the mean of three experiments in triplicate and were expressed as means ± SD. only descriptive statistics were done in the text. [b] Telomerase supercoiling activity. [c] Used as a positive control. [d] Not observed in the tested concentration range. [e] > 100 μM.

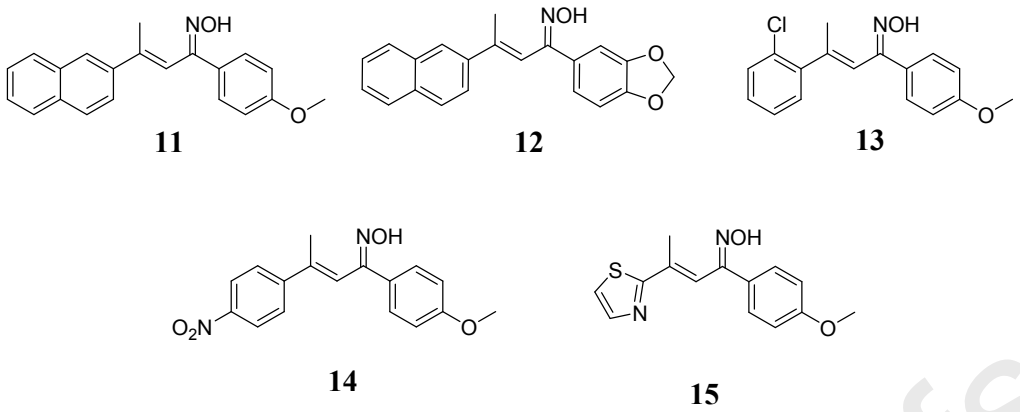

Figure 6. The structure of compounds **11**~**15**

Table 3. Inhibitory activity of compounds **11**~**15** against SGC-7901, A375, SMMC-7721, MGC-803, GES cell lines [a] and telomerase [b]

compound	IC_{50}（μM）					
	SGC-7901	A375	SMMC-7721	SGC-803	GES	telomerase
11	2.84±0.95	4.49±1.87	7.01±1.83	10.56±2.25	10.79±2.04	0.99±0.21
12	10.00±1.09	7.24±3.85	23.50±2.27	18.42±1.42	32.32±4.03	1.58±0.29
13	18.36±2.16	>100	33.94±1.04	20.53±3.27	14.40±0.99	5.57±0.84
14	33.26±3.57	17.48±4.23	14.54±0.77	23.90±4.04	17.56±1.68	-[d]
15	40.67±4.66	15.58±2.35	15.01±1.07	18.29±3.64	10.28±3.62	6.33±0.59
ADR[c]	0.62±0.21	0.75±0.23	0.55±0.36	0.84±0.094	0.69±0.30	-
STSN[c]	-	-	-	-	-	6.98±1.59
BIBR1532[c]	-	-	-	-	-	0.32±0.07

[a] The data represented the mean of three experiments in triplicate and were expressed as means ± SD. only descriptive statistics were done in the text. [b] Telomerase supercoiling activity. [c] Used as a positive control. [d] >100 μM.

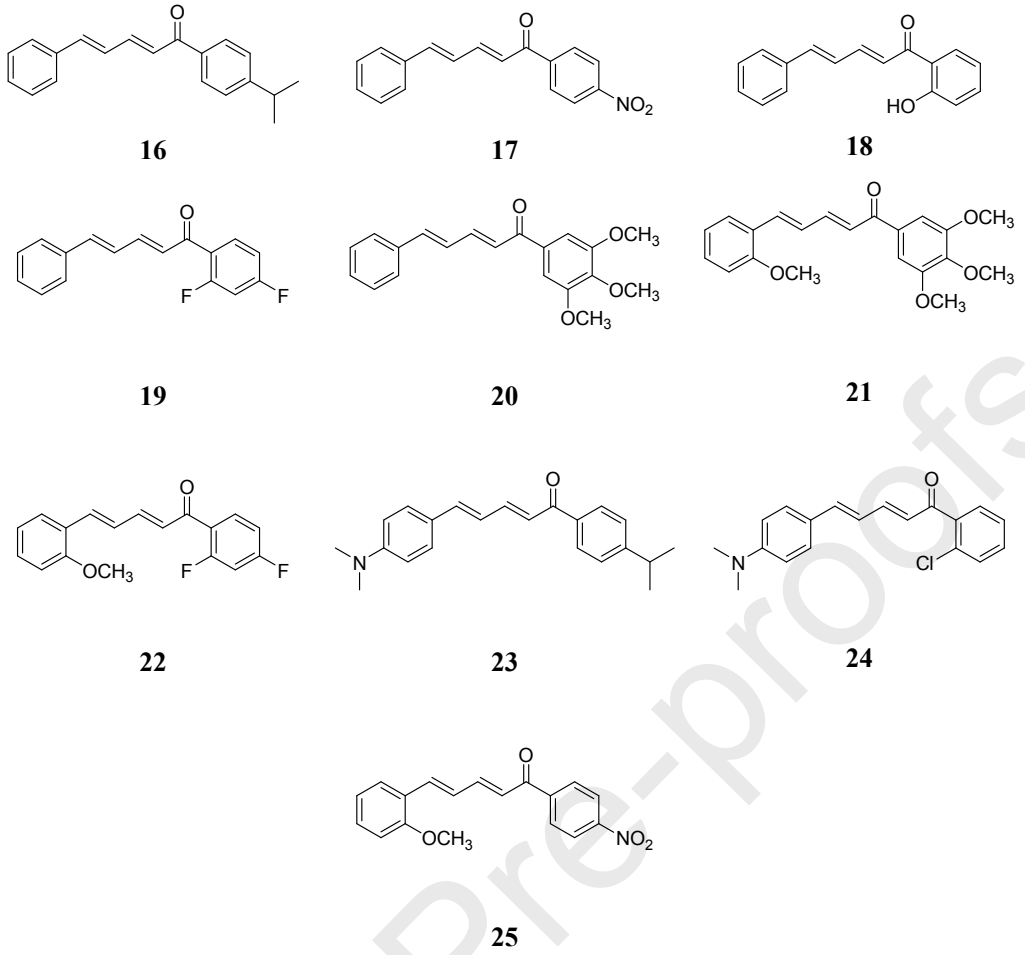

Figure 7. The structure of compounds **16**~**25**

Table 4. Inhibitory activities of compounds **16**~**25** against SGC-7901, A375, SMMC-7721, MGC-803, GES cell lines[a] and telomerase [b]

compound	IC_{50}（μM）					
	SGC-7901	A375	SMMC-7721	MGC-803	GES	telomerase
16	>100	>100	>100	>100	>100	-[e]
17	>100	>100	>100	>100	>100	ND[d]
18	>100	63.67±3.00	>100	>100	>100	-
19	23.02±3.02	20.23±4.39	>100	>100	>100	-
20	61.54±4.74	23.67±0.48	77.36±2.23	14.64±0.47	50±4.68	ND
21	6.41±1.63	2.46±0.73	2.98±0.50	1.56±0.16	1.90±0.82	8.12±1.01
22	82.55±2.76	73.91±4.34	51.72±1.95	81.13±3.91	>100	7.07±1.22
23	>100	>100	>100	>100	>100	-
24	>100	>100	>100	>100	>100	-
25	>100	>100	>100	>100	>100	-
ADR[c]	0.62±0.21	0.75±0.23	0.55±0.36	0.84±0.094	0.69±0.30	-
STSN[c]	-	-	-	-	-	6.98±1.59
BIBR1532[c]	-	-	-	-	-	0.32±0.07

[a] The data represented the mean of three experiments in triplicate and were expressed as means ± SD. only descriptive statistics were done in the text. [b] Telomerase supercoiling activity. [c] Used as a positive control. [d] Not observed in the tested concentration range. [e] >100 μM.

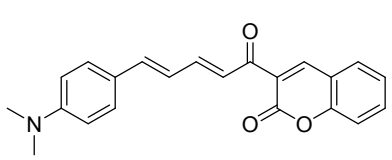

26

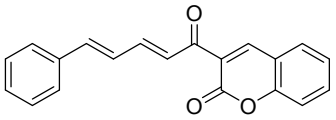

27

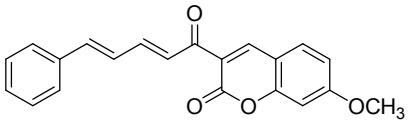

28

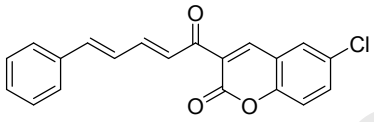

29

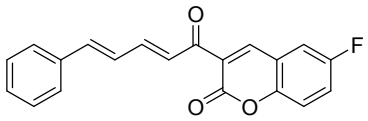

30

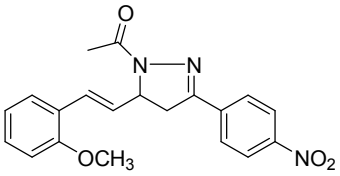

31

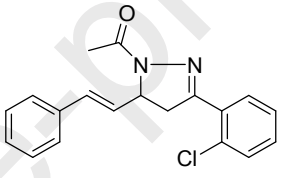

32

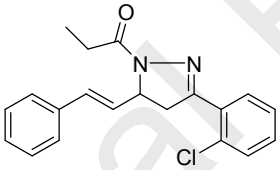

33

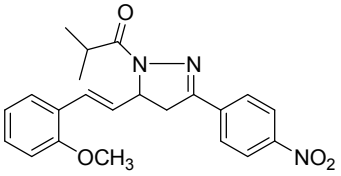

34

Figure 8. The structure of compounds **26**~**34**

Table 5. Inhibitory activities of the compounds **26~34** against SGC-7901, A375, SMMC-7721, MGC-803, GES cell lines[a] and telomerase [b]

compound	IC_{50}（μM）					
	SGC-7901	A375	SMMC-7721	MGC-803	GES	telomerase
26	>100	>100	>100	>100	>100	-[d]
27	>100	>100	>100	>100	>100	-
28	>100	>100	>100	>100	>100	-
29	>100	>100	>100	>100	>100	-
30	>100	>100	>100	>100	>100	-
31	>100	>100	>100	>100	>100	-
32	>100	>100	17.02±4.72	>100	>100	-
33	>100	>100	>100	>100	>100	6.33 ±0.89
34	>100	>100	>100	>100	>100	-
ADR[c]	0.62±0.21	0.75±0.23	0.55±0.36	0.84±0.094	0.69±0.30	-
STSN[c]	-	-	-	-	-	6.98±1.59
BIBR1532[c]	-	-	-	-	-	0.32±0.07

[a] The data represented the mean of three experiments in triplicate and were expressed as means ± SD. only descriptive statistics were done in the text. [b] Telomerase supercoiling activity. [c] Used as a positive control. [d] ＞100 μM.

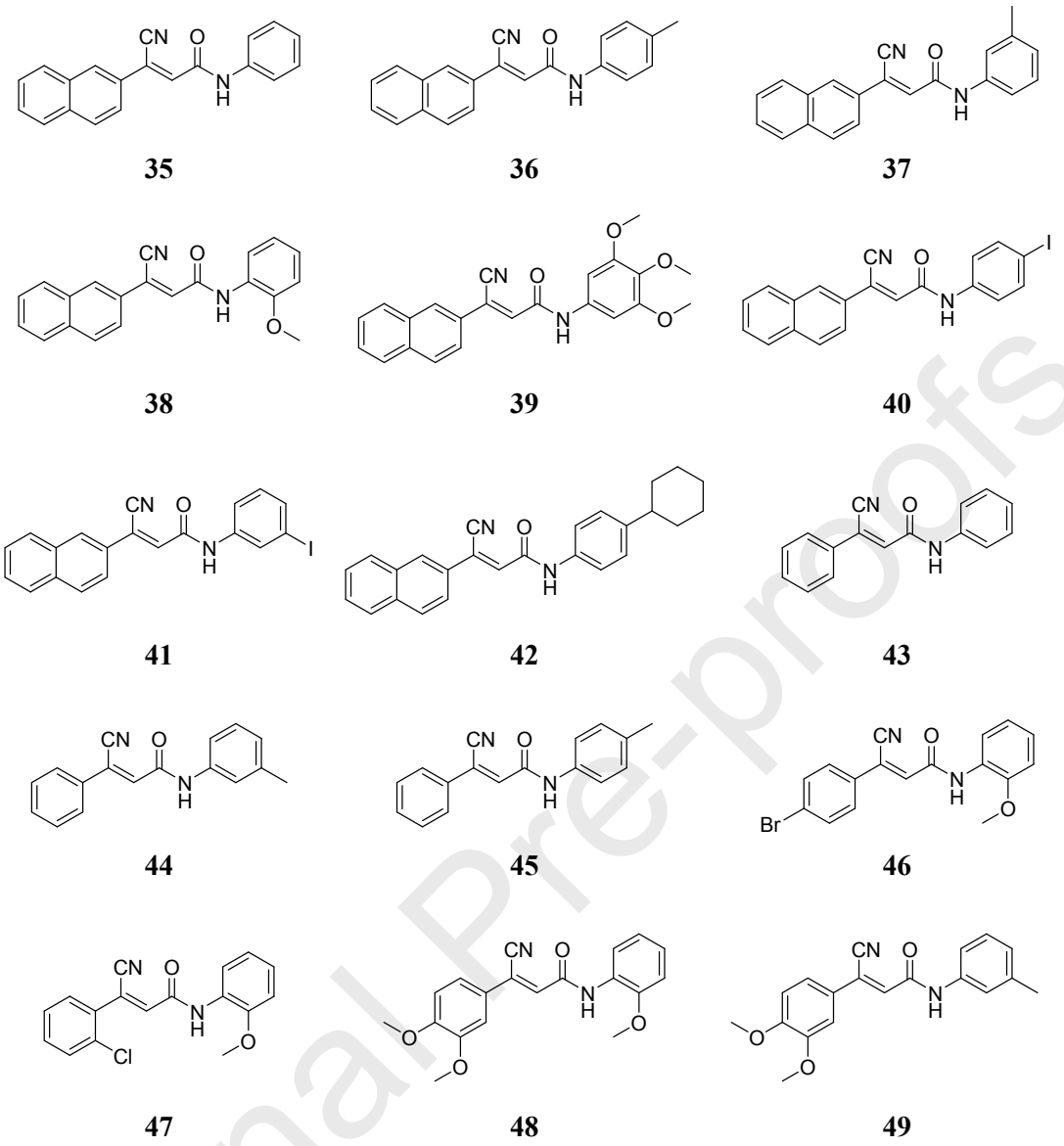

Figure 9. The structure of compounds **35**~**49**

Table 6. Inhibitory activities of the compounds **35**~**49** against SGC-7901, A375, SMMC-7721, MGC-803, GES cell lines [a] and telomerase [b]

compound	IC_{50}（μM）					
	SGC-7901	A375	SMMC-7721	MGC-803	GES	telomerase
35	27.47±2.86	>100	>100	30.58±2.99	>100	-[e]
36	>100	66.99±3.10	>100	80.08±2.65	>100	ND
37	>100	52.43±1.94	>100	77.08±2.71	>100	-
38	9.33±2.34	5.64±3.11	10.57±1.89	17.82±2.43	88.81±3.33	2.01±0.45
39	>100	>100	>100	14.14±2.47	>100	0.62±0.12
40	>100	>100	>100	26.54±0.34	>100	2.38±0.77
41	>100	>100	>100	>100	>100	-
42	>100	>100	35.87±0.87	>100	>100	0.81±0.19
43	>100	>100	55.18±3.42	71.99±4.17	>100	ND[d]
44	>100	33.36±0.82	55.79±2.23	>100	>100	ND
45	>100	>100	>100	>100	>100	ND
46	>100	>100	>100	>100	>100	ND
47	>100	>100	>100	>100	>100	-
48	>100	>100	>100	30.30±2.11	>100	3.07±0.28
49	>100	>100	>100	>100	>100	-
ADR[c]	0.62±0.21	0.75±0.23	0.55±0.36	0.84±0.094	0.69±0.30	-
STSN[c]	-	-	-	-	-	6.98±1.59
BIBR1532[c]	-	-	-	-	-	0.32±0.07

[a] The data represented the mean of three experiments in triplicate and were expressed as means ± SD. only descriptive statistics were done in the text. [b] Telomerase supercoiling activity. [c] Used as a positive control. [d] Not observed in the tested concentration range. [e] > 100 μM

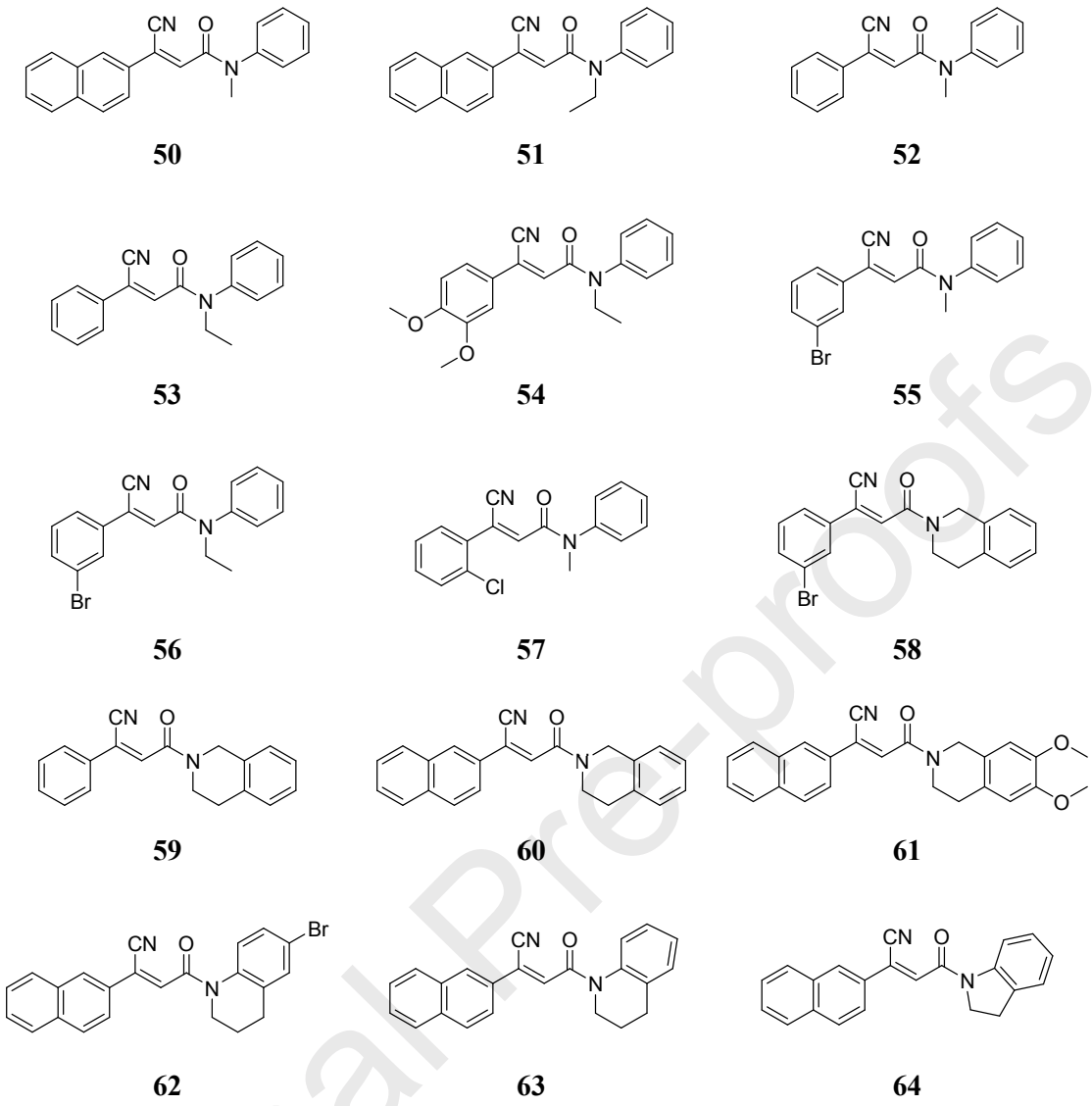

Figure 10. The structure of compounds **50~64**

Table 7. Inhibitory activities of the compounds **50~64** against SGC-7901, A375, SMMC-7721, MGC-803, GES cell lines[a] and telomerase [b]

compound	IC_{50}（μM）					
	SGC-7901	A375	SMMC-7721	MGC-803	GES	telomerase
50	39.59±3.71	10.86±1.27	65.86±2.85	13.60±0.50	>100	8.11±1.51
51	39.61±2.28	11.58±0.77	47.51±2.88	15.73±3.83	>100	-[e]
52	13.16±2.98	16.44±3.26	35.16±4.61	>100	>100	-
53	34.13±1.94	>100	15.81±3.27	19.10±0.66	>100	-
54	>100	44.55±1.28	>100	65.85±4.22	>100	-
55	10.21±2.06	3.36±1.09	11.59±2.95	9.36±2.43	>100	6.19±1.20
56	4.85±1.05	1.87±0.33	5.39±0.95	11.16±3.81	>100	1.41 ± 0.17
57	6.68±1.42	2.88±1.07	3.67±2.15	14.80±3.23	>100	0.99±0.32
58	14.67±1.66	16.77±2.25	11.49±1.01	33.29±4.64	>100	3.17±0.95
59	3.13±1.22	9.09±2.40	7.72±3.63	6.23±1.58	>100	0.93 ± 0.06
60	>100	>100	70.77±4.32	60.69±3.14	>100	ND[d]
61	>100	21.09±0.13	>100	>100	>100	1.06 ± 0.21
62	>100	24.13±0.89	>100	13.09±0.15	95.70±0.42	4.11 ± 1.30
63	>100	>100	>100	39.12	>100	6.01 ± 1.29
64	>100	17.65±0.47	>100	60.12±0.81	>100	25.50±1.99
ADR[c]	0.62±0.21	0.75±0.23	0.55±0.36	0.84±0.094	0.69±0.30	-
STSN[c]	-	-	-	-	-	6.98±1.59
BIBR1532[c]	-	-	-	-	-	0.32±0.07

[a] The data represented the mean of three experiments in triplicate and were expressed as means ± SD. only descriptive statistics were done in the text. [b] Telomerase supercoiling activity. [c] Used as a positive control. [d] Not observed in the tested concentration range. [e] >100 μM.

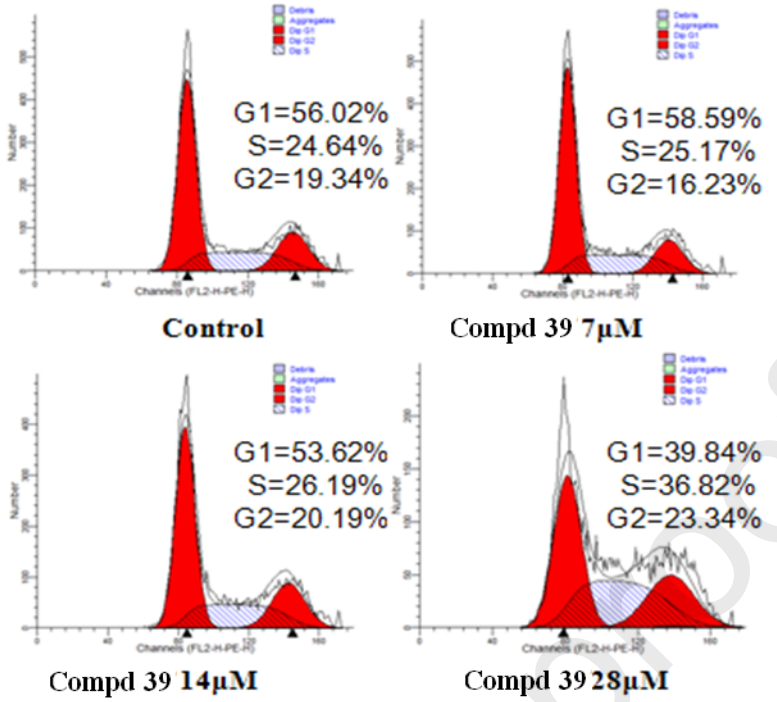

Figure 11. Effect of compound **39** on MGC-803 cells cycle

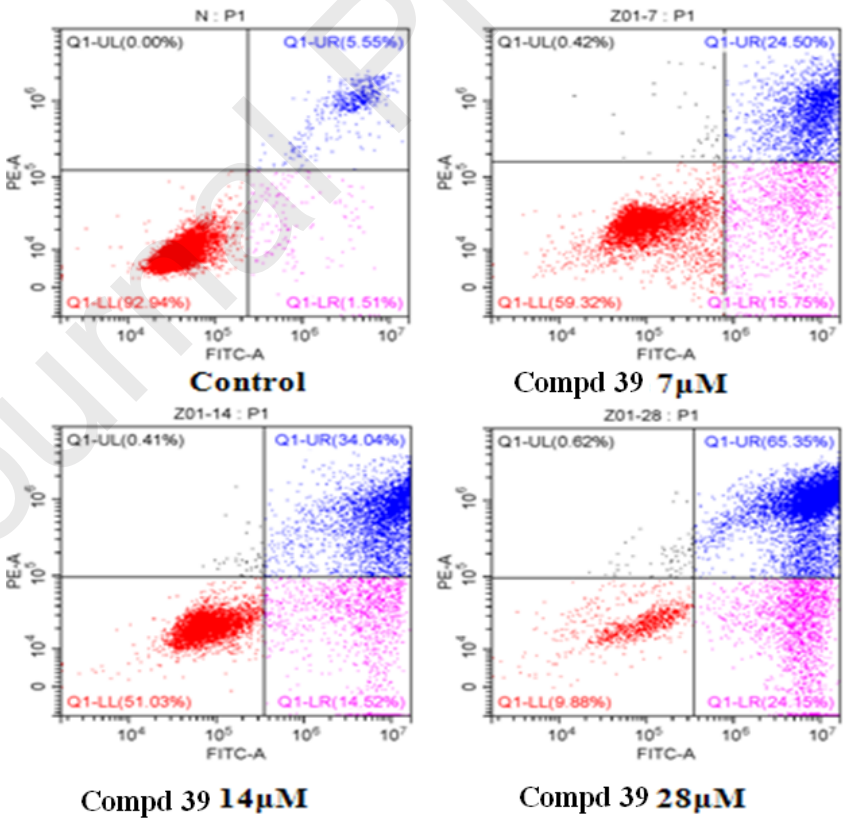

Figure 12. Effect of compound **39** on MGC-803 cells apoptosis

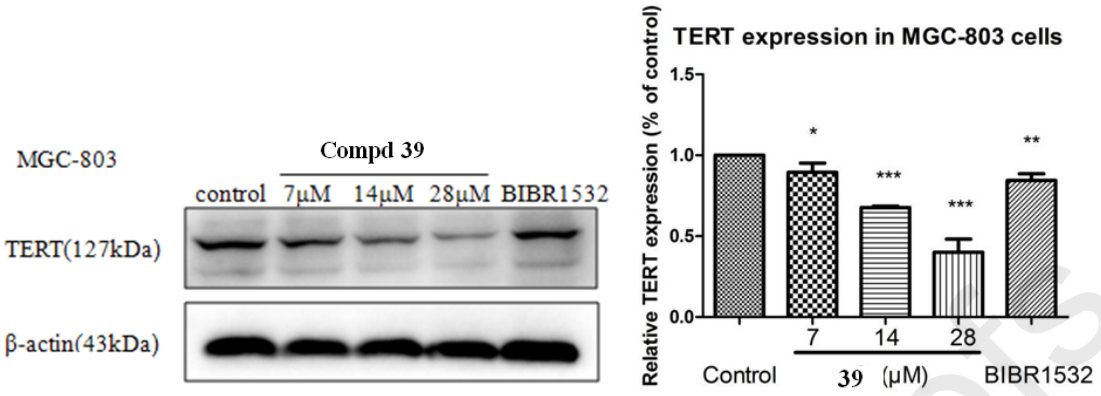

(*p<0.05，** p<0.01，*** p<0.001)

Figure 13. Effect of compound **39** on TERT protein expression

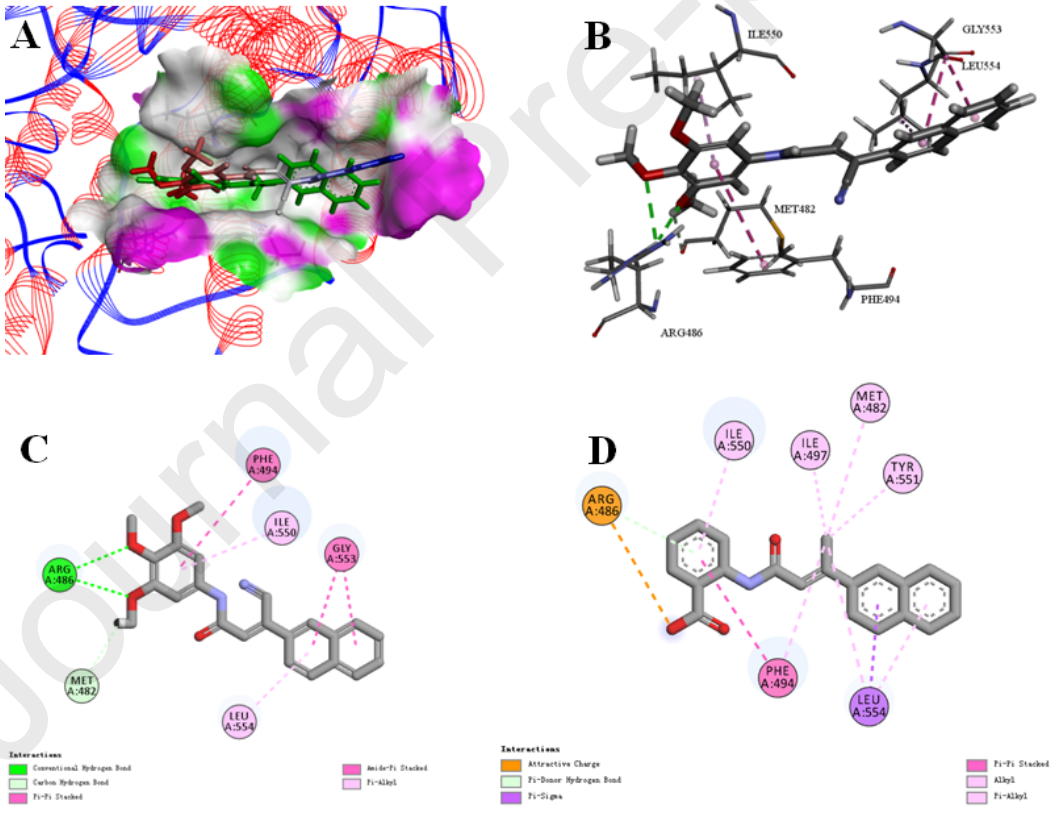

Figure 14. (**A**) Binding site (PDB: 5CQG) of TERT, BIBR1532 (green) and compound **39** (red with blue). (**B**) Binding mode(three-dimensional image) of compound **39** to TERT. (**C**) Binding mode (tow-dimensional image) of compound **39** to TERT. (**D**) Binding form (tow-dimensional image) of BIBR1532 to TERT.

Declaration of Interest Statement

Design, synthesis and SARs of novel telomerase inhibitors based on BIBR1532

Chao Liu[b,#], Hua Zhou [a,#], Fei Hu Cheng [a,*], Xin Hua Liu[a,*]

[a] *School of Pharmacy, Anhui Medical University, Hefei, 230032, P. R. China*

[b] *School of chemistry, Suzhou University, Suzhou, 234000, P. R. China*

All authors have contributed to the work, have read the manuscript and have agreed to be listed as authors. The submitted manuscript has not been published elsewhere and nor is it currently under review by another publication. No potential conflict of interest relevant to this article.

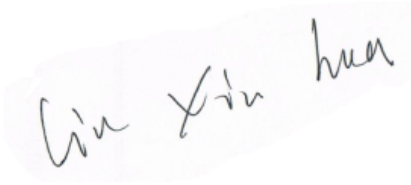

10/05/2020

Design, synthesis and SARs of novel telomerase inhibitors based on BIBR1532

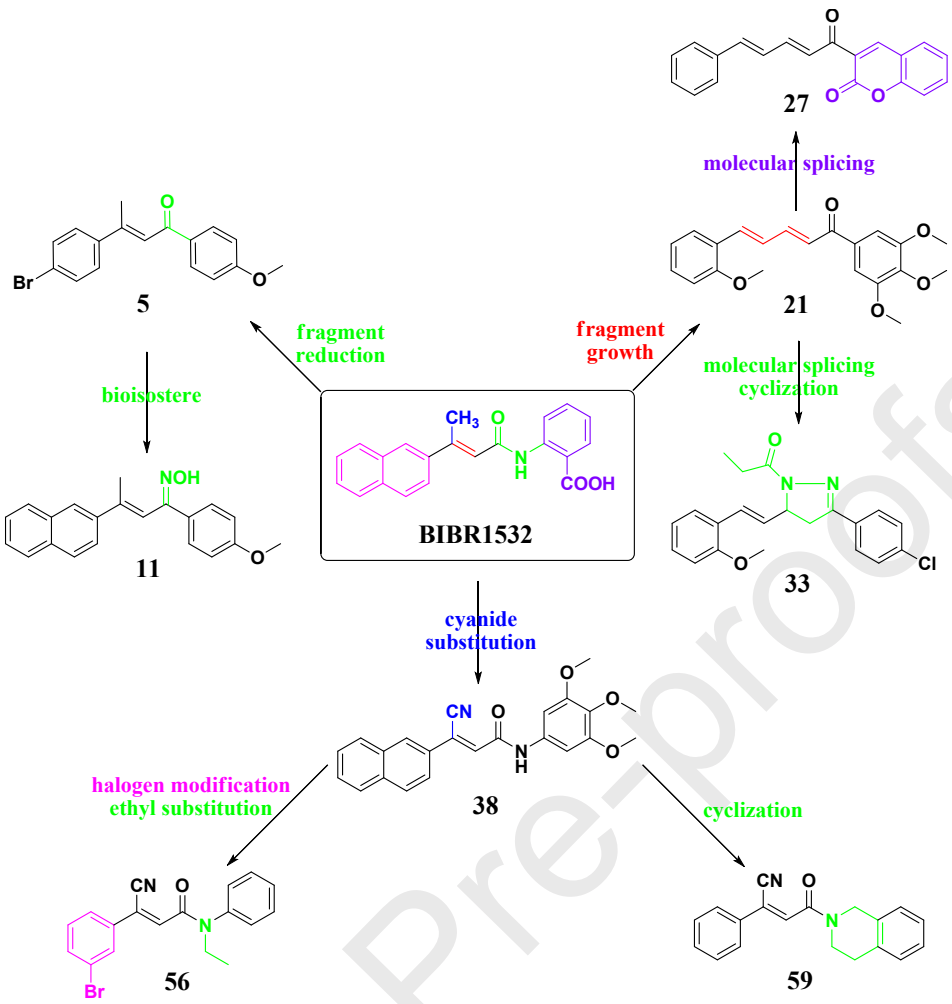

With the aim to discover high efficiency telomerase inhibitors, based on rational design and follow-up strategy, total of 64 new BIBR1532 derivatives were designed. Many of these compounds showed good inhibitory activity against cancer cells and telomerase. Their structure-activity relationships were well summarized on basis of different design strategies.

Highlights

► New BIBR1532 derivatives were designed and synthesized.

► Clear structure-activity relationships were summarized.

► Preliminary mechanism as telomerase inhibitor action was discovered.